A temperature sensor based on the splicing of a core offset multi-mode fiber with two single mode fibers*

FU Xing-hu (付兴虎)[1,2]**, **LIU Qin** (刘琴)[1], **XIU Yan-li** (修艳丽)[1], **XIE Hai-yang** (谢海洋)[1], **YANG Chuan-qing** (杨传庆)[1], **ZHANG Shun-yang** (张顺杨)[1], **FU Guang-wei** (付广伟)[1,2], **and BI Wei-hong** (毕卫红)[1,2]

1. School of Information Science and Engineering, Yanshan University, Qinhuangdao 066004, China

2. The Key Laboratory for Special Fiber and Fiber Sensor of Hebei Province, Qinhuangdao 066004, China

(Received 10 August 2015; Revised 5 September 2015)

In this paper, a temperature sensor based on the splicing of a core offset multi-mode fiber with two single mode fibers is proposed and demonstrated experimentally. The temperature sensing principle is analyzed and related experiment is performed. By controlling the core offset and splicing length of the specialty multi-mode fiber (SMMF), two sensors with different temperature sensing properties are obtained, and experimental results show that the temperature sensitivity can be up to 48.76 pm/°C in the range of 25—95 °C. Moreover, it has many advantages, including small size, high sensitivity, and simple structure. So it can be used in potential temperature sensing applications, such as industrial production, biomedical science, power electronics, and so on.

Document code: A **Article ID:** 1673-1905(2015)06-0434-4

DOI 10.1007/s11801-015-5155-2

Recently, fiber temperature sensor has been used in many fields[1-3], including transformer substation, petroleum pipeline, and fire safety. Moreover, based on the features of high sensitivity, fast response, and small dimension, some scientists researched different fiber structures for temperature measurement, such as fiber Bragg gratings[4,5], Brillouin optical time domain reflectometer[6,7], tapered fiber[8,9] and so on. For example, Shuo Yuan et al[10] proposed an optical fiber high temperature sensor, which was fabricated by cascading two spherical-shape structures. Jiajun Wang et al[11] analyzed a polished C-plane sapphire fiber temperature sensor, and a sub-micrometer thick zirconium dioxide film was deposited on the sapphire fiber to form a Fabry-Perot interferometric sensor. However, these complicated sensor structures are difficult to fabricate. Thereby, a simple fiber temperature sensor is necessary.

In this paper, a temperature sensor based on the splicing of a core offset multi-mode fiber with two single mode fibers (SMF, Corning SMF-28e) is proposed. The temperature sensing principle is analyzed and testing experiment is performed. By changing the core offset and splicing length of specialty multi-mode fiber (SMMF), the experimental results are discussed in detail. In the temperature range of 25—95 °C, this sensor has good temperature measurement performance.

The cross section of SMMF is shown in Fig.1. It is composed of pure silica core and glass cladding, which is fabricated by Yangtze Optical Fiber and Cable Joint Stock Limited Company. The fiber core refractive index is greater than the cladding refractive index. Fiber core and cladding diameters are 105 μm and 125 μm, respectively. A number of high order core modes will be stimulated in SMMF due to its lager core diameter by core offset method. Then the interference between core and cladding modes can be achieved.

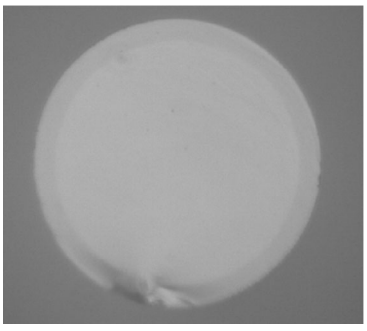

Fig.1 The cross section of SMMF

Based on this interference principle, the schematic diagram of the proposed SMMF sensor is shown in Fig.2.

In Fig.2, the SMMF is spliced between SMF1 and SMF2 by using the fusion splicer (FITEL S178). By adjusting the discharge current, discharge time and dis-

* This work has been supported by the National Natural Science Foundation of China (Nos.61205068 and 61475133), College Youth Talent Project of Hebei Province (No.BJ2014057), "Xin Rui Gong Cheng" Talent Project and the Excellent Youth Funds for School of Information Science and Engineering of Yanshan University (No.2014201).

** E-mail: fuxinghu@ysu.edu.cn

placement parameters of the fusion splicer, the different core offsets can be obtained. Thus, different miniature Mach-Zehnder interferometers can be fabricated. The splicing point photomicrographs between different fibers are shown in Fig.3.

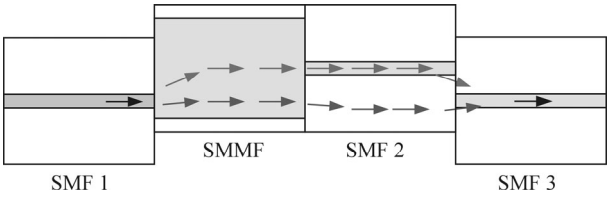

Fig.2 Schematic diagram of the cascaded SMMF sensor

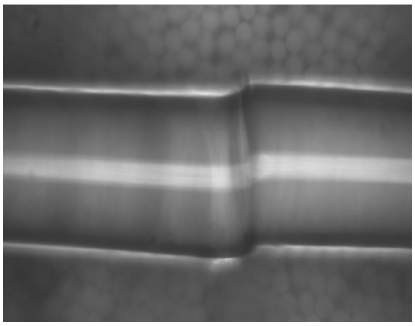

(a) SMF1 and SMMF

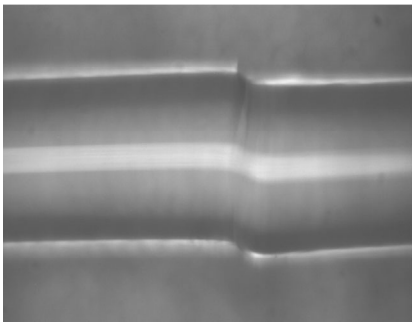

(b) SMF2 and SMF3

Fig.3 Splicing point photomicrographs between different fibers

For the miniature Mach-Zehnder interferometer, the sensing principle is as follows.

The transmission light in SMF1 will be coupled into SMMF core, and different transmission modes will be excited. Because of the mismatch mode field between different fibers, the output beam of SMMF is mainly divided into two parts which propagate in SMF2 core and cladding separately. At this time, some transmission modes will be excited in SMF2 cladding. In order to simplify the analysis, only the main transmission mode with the largest energy in SMF2 cladding will be considered. Therefore, the transmission light in fiber core and cladding can be regarded as the reference and signal arms, respectively. When two beams reach SMF3, the interference phenomenon happens.

Based on double-beam interference principle[12], the phase delay of the two different modes and the central wavelength satisfy the equation of

$$\varphi = \frac{2\pi\left(n_{\text{eff}}^{\text{core}} - n_{\text{eff}}^{\text{clad}}\right)L}{\lambda} = \frac{2\pi\Delta n_{\text{eff}} L}{\lambda}, \tag{1}$$

$$\lambda_m = \frac{\Delta n_{\text{eff}} L}{m}, \tag{2}$$

where $n_{\text{eff}}^{\text{core}}$ and $n_{\text{eff}}^{\text{clad}}$ are the effective refractive indices of core and cladding modes in SMF, respectively. Δn_{eff} is the difference of them, λ is the spatial wavelength of fringe, λ_m is the central wavelength of the m-th order interference fringe, and L is the interference length, namely the total length of SMMF and SMF2. As can be seen from Eq.(1) and Eq.(2), the SMMF length will affect the peak wavelength of interference fringe. Moreover, the core offset also affects the fringe visibility and free spectral range (FSR) of interference spectrum.

With the environmental temperature changing, the refractive index and geometry structure of fiber will change due to the thermo-optic effect and thermal expansion effect. It leads to the variation of phase difference between core mode and cladding mode. The interference spectrum will also shift. Therefore, the wavelength shift with temperature changing can be deduced from Eq.(2), which is expressed as

$$\Delta\lambda_m = \frac{\Delta L\Delta n_{\text{eff}} + L\Delta n}{m}, \tag{3}$$

where $\Delta\lambda_m$ is the central wavelength shift of the m-th order interference fringe, and Δn_{eff} is the effective refractive index difference between core mode and cladding mode. With the temperature increasing, thermal expansion effect and thermo-optic effect will be produced in fiber. Moreover, the thermal expansion effect will lead to little change for the fiber length ΔL. The change of effective refractive index difference Δn is mainly affected by thermo-optic effect. Both changes will lead to transmission spectrum shifts, so the external temperature can be detected by measuring the interference fringe shift.

In order to investigate the temperature performance of this sensor, a related experiment is performed. The experimental setup is shown in Fig.4. An amplified spontaneous emission (ASE) optical source ranging from 1 520 nm to 1 610 nm, an optical spectrum analyzer (OSA, YOKOGAWA AQ6375) and a temperature controlled cabinet (WHL-30B) are used to test the temperature sensor.

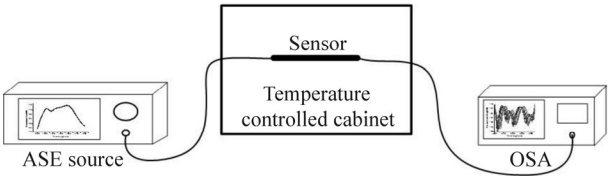

Fig.4 Experimental setup for temperature measurement

During the experiment, the proposed SMMF sensor is placed in the temperature controlled cabinet. The interference spectrum is recorded and investigated experimentally within 25—95 °C with an interval of 10 °C. In order to further study the temperature performance, some experiments are performed based on different core offsets and splicing lengths of SMMF. The following two sensors are taken as examples to illustrate the idea.

When the SMMF length is 25 mm, the SMF2 length is 40 mm, the core offset is 10.5 μm between SMF1 and SMMF, and the core offset is 9.1 μm between SMF2 and SMF3, the interference spectra of the first sensor with different temperatures are depicted in Fig.5.

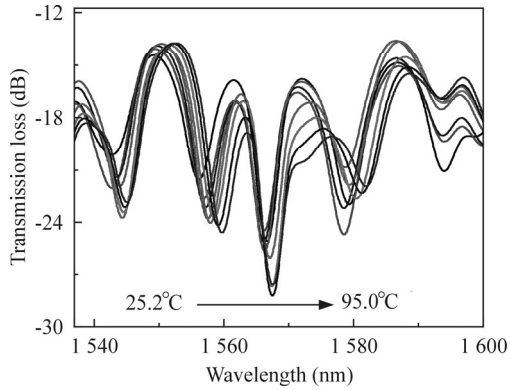

Fig.5 Interference spectra corresponding to different temperatures for the first sensor

In Fig.5, we can see that with the temperature increasing, the interference spectra have obvious shift towards long wavelength. In order to illustrate the changes of interference spectra with different temperatures more directly, the wavelengths near 1 560 nm in spectra are selected as the observation points. The temperature response characteristic of the interference spectrum is shown in Fig.6.

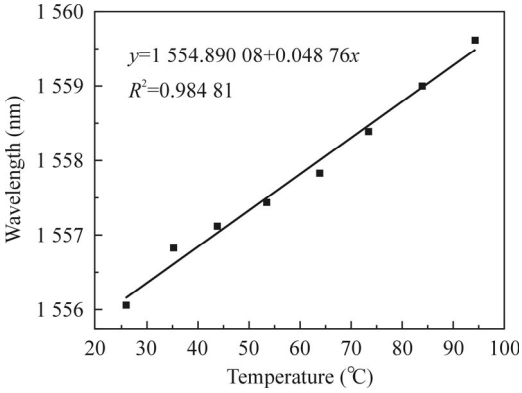

Fig.6 Temperature response characteristic of the interference spectrum for the first sensor

As shown in Fig.6, it exhibits high sensitivity to temperature, almost 48.76 pm/°C. When the SMMF length is 20 mm, the SMF2 length is 20 mm, the core offset is 10.3 μm between SMF1 and SMMF, and the core offset is 5.2 μm between SMF2 and SMF3, the interference spectra of the second sensor with different temperatures are depicted in Fig.7.

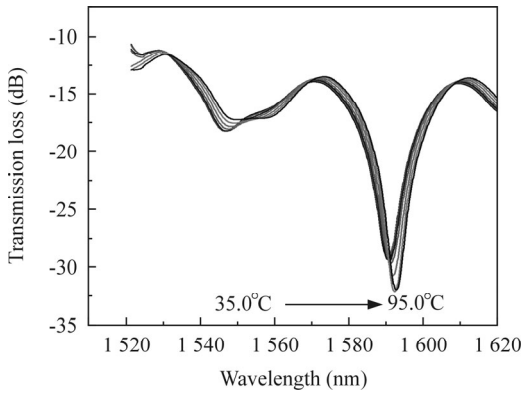

Fig.7 Interference spectra corresponding to different temperatures for the second sensor

Similarly, we can see that with the temperature increasing, the interference spectra have obvious shift towards long wavelength in Fig.7. The wavelengths near 1 580 nm in the spectra are selected as the observation points. So we can obtain the temperature response characteristic curve as shown in Fig.8.

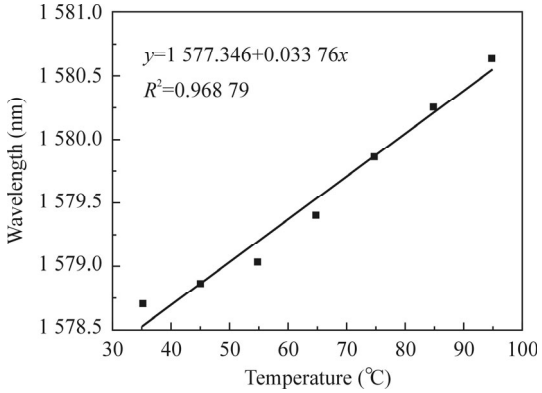

Fig.8 Temperature response characteristic of the interference spectrum for the second sensor

As shown in Fig.8, it exhibits high sensitivity to temperature, almost 33.76 pm/°C. For these two sensors, there is perfect temperature performance. For different core offsets and splicing lengths, different transmission modes are excited. Due to the thermal-optic effect and thermal expansion effect in fiber, the effective refractive index difference Δn increases as temperature increasing. Through Eq.(3), the wavelength shifts of different dips also have direct relationship with Δn. Thereby, by measuring the wavelength shift of observation point, the variation of the external temperature can be determined.

This work describes a novel temperature fiber sensor based on SMMF. The sensing mechanism of it is analyzed in detail and then its temperature characteristic is experimentally demonstrated. Experimental results show that the temperature sensitivity can be up to 48.76 pm/°C

in the range of 25—95 °C. Moreover, it has many features, including small size, high sensitivity, and simple structure. So it is expected to be applied in temperature sensing fields, such as industrial production, biomedical science, power electronics, and so on.

References

[1] T. Li, Y.T. Dai and Q.C. Zhao, Journal of Optoelectronics·Laser **25**, 625 (2014). (in Chinese)

[2] S.L Zhang, Z.W. Zhao, N. Chen, F.F. Pang, Z.Y. Chen, Y.Q. Liu and T.Y. Wang, Optics Letters **40**, 1362 (2015).

[3] W.H. Bi, C.Q. Zhu, X.H. Fu, G.W. Fu and B.J. Zhang, Journal of Optoelectronics·Laser **25**, 1443 (2014). (in Chinese)

[4] Z.Y. Bai, W.G. Zhang, S.C. Gao, H. Zhang, L. Wang and F. Liu, Optical Fiber Technology **21**, 110 (2015).

[5] M. Ding, M.N. Zervas and G. Brambilla, Optics Express **19**, 15621 (2011).

[6] Y.X. Zhang, X.L. Wu, Z.F. Ying and X.P Zhang, Electronics Letters **50**, 1014 (2014).

[7] S.M. Maughan, H.H. Kee and T.P. Newson, Measurement Science and Technology **12**, 834 (2001).

[8] X.D. Wen, T.G. Ning, H.D. You, J. Li, T. Feng, L. Pei and W. Jian, Optoelectronics Letters **9**, 325 (2013).

[9] F.B. Mej´ıa, C.R. Biazoli and C.M.B. Cordeiro, Optics Express **22**, 30432 (2014).

[10] S. Yuan, Z.R.Tong, J.F. Zhao, W.H. Zhang and Y. Cao, Optics Communications **332**, 154 (2014).

[11] J.J. Wang, E.M. Lally, X.P. Wang, J.M. Gong, G. Pickrell and A.B. Wang, Applied Optics **51**, 2129 (2012).

[12] H.B. Gan, Z. Chen, J. Zhang, H.B. Gan, J.Y. Tang, Y.H. Luo, J.H. Yu, H.H. Lu and H.Y. Guang, Journal of Optoelectronics·Laser **26**, 633 (2015). (in Chinese)